JOINT INSTITUTE FOR NUCLEAR RESEARCH

Department of Raman spectroscopy, Frank Laboratory of Neutron physics

FINAL REPORT ON THE START PROGRAMME

Preparation of Two-Dimensional Materials and characterization by Raman Spectroscopy: Graphene and MoS_2

Supervisor:

Prof.Dr/Grigory Arzumanyan

Student:

Mohamed Moustafa Mahmoud Hmeda

Egypt, Fayoum University

Participation period:

February 15 – March 28,

START Winter Session 2026

Dubna 2026

Table of Contents

1. Abstract

Raman spectroscopy is a powerful, non-destructive tool for characterizing two-dimensional materials such as graphene and MoS_2. Graphene exhibits prominent G, D, and 2D bands, sensitive to layer number, defects, strain, and doping, whereas MoS_2 shows E_2g^1 and A_1g modes that reflect layer thickness, phase, and interlayer interactions. In heterostructures, Raman reveals charge transfer, strain, and interface coupling, producing shifts distinct from the constituent materials. Comparative Raman studies elucidate resonant and double-resonance processes, defect distributions, and phase behavior, providing critical insight for device design. Understanding these Raman signatures allows accurate identification of layer number, defects, doping, and interfacial effects, making Raman spectroscopy indispensable for probing the structural and electronic properties of graphene, MoS_2, and their van der Waals heterostructures

2. Introduction

Raman spectroscopy is a vibrational spectroscopic technique based on the inelastic scattering of monochromatic light (the Raman effect), in which only a small fraction of photons undergoes a measurable frequency shift after interacting with molecular vibrations. This shift encodes highly specific structural information, making Raman spectroscopy a powerful molecular fingerprinting tool for a wide range of materials and environments[1-3]. The technique has become increasingly important in analytical chemistry, life sciences, materials science, and environmental monitoring due to its non-destructive nature, minimal sample preparation requirements, and compatibility with aqueous systems[4-7]. The fundamental principle of Raman spectroscopy arises when incident light excites molecules to a virtual energy state; as the molecules relax, the scattered photons exhibit frequency shifts corresponding to vibrational energy differences. These shifts provide detailed information about bond types, molecular symmetry, chemical composition, and structural changes within the sample[8-11]. Two-dimensional (2D) materials have emerged as a transformative class of materials due to their unique structural, electronic, and optical properties. Their atomic-scale thickness and high surface-to-volume ratio result in behaviors that differ significantly from their bulk counterparts, making them promising candidates for next-generation electronic, photonic, and sensing devices. Among these materials, graphene and molybdenum disulfide (MoS_2) are particularly prominent[12-16]. Graphene, a single layer of sp^2-hybridized carbon atoms arranged in a honeycomb lattice, exhibits exceptional electrical conductivity, mechanical strength, thermal stability, and optical transparency. Its zero bandgap and linear energy dispersion enable high carrier mobility and tunable optical properties, making it a benchmark material in 2D materials research. Graphene can be synthesized using various methods, including Plasma-Enhanced Chemical Vapor Deposition (PECVD), which enables controlled growth at relatively lower temperatures and offers advantages in scalability and film uniformity. On the other hand, MoS_2, a transition-metal dichalcogenide, exhibits a layer-dependent bandgap, transitioning from an indirect bandgap in the bulk to a direct bandgap in the monolayer form. This semiconducting behavior, along with strong excitonic effects and high on/off current ratios in field-effect transistors, makes MoS_2 highly complementary to graphene in

electronic and optoelectronic applications. Raman spectroscopy has become an indispensable tool for the characterization of 2D materials, as it probes vibrational modes in a non-destructive manner and provides insight into crystal structure, layer number, strain, doping, defects, and phase. In graphene, the main Raman features include the G, D, and 2D bands. The G band originates from in-plane vibrations of sp^2 carbon atoms, while the D band is associated with defects or disorder. The 2D band, a second-order process, is highly sensitive to the number of layers, stacking order, and electronic structure. Variations in peak position, width, and intensity can indicate strain, doping levels, or chemical modifications. For MoS_2, the characteristic Raman modes are the E_2g^1 (in-plane) and A_1g (out-of-plane) vibrations. The frequency difference between these modes is strongly dependent on the number of layers, providing a simple and reliable method for thickness identification. Raman spectroscopy can also detect defect-induced modes, intervalley scattering, and phase transitions, such as the transformation from the semiconducting 2H phase to the metallic 1T phase. Additionally, resonant Raman scattering in MoS_2 is influenced by excitonic transitions, which can be tuned through laser wavelength, temperature, and strain. Beyond individual materials, Raman spectroscopy plays a crucial role in studying heterostructures formed by stacking different 2D materials.[17-21].

3. Materials and Methods

3.1 Electropolishing Method (as substrate for graphene)

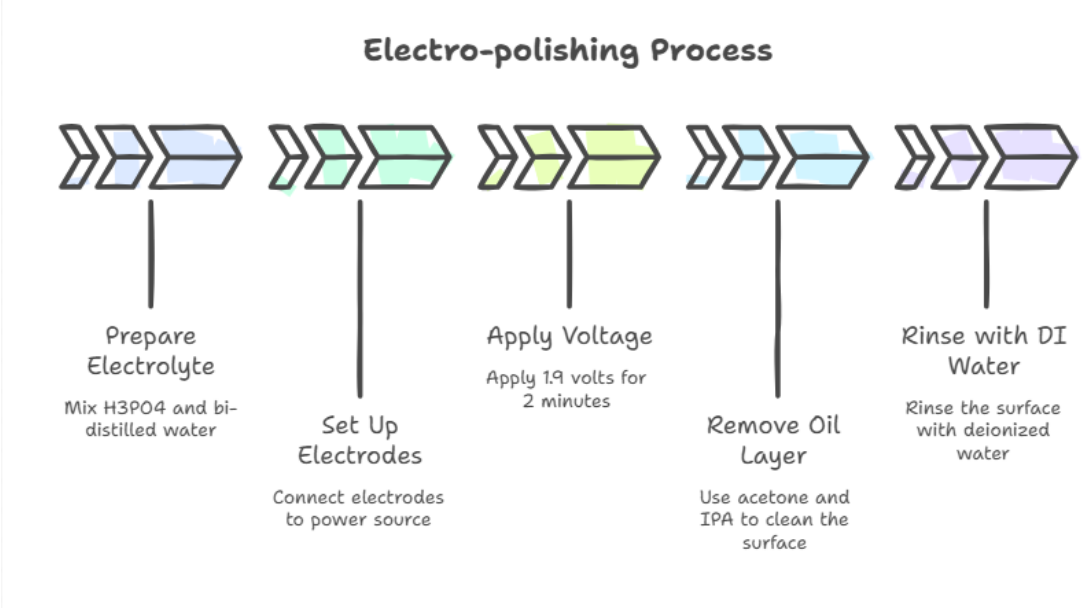

Scheme (1) is a schematic diagram that illustrates the electropolishing process used to prepare the Cu foil surface before further experiments.

The schematic diagram illustrates the electro-polishing process used to prepare the Cu foil surface before further experiments. First, the electrolyte solution is prepared by mixing phosphoric acid (H_3PO_4) with bi-distilled water. This solution acts as the conductive medium for the electrochemical polishing process. Next, the electrodes are arranged in the electrochemical cell. The copper foil is connected as the positive electrode (anode), while stainless steel is used as the negative electrode (cathode). Both electrodes are connected to a power supply. After setting up the system, a constant voltage of 1.9 V is applied for 2 minutes. During this step, controlled electrochemical dissolution occurs at the copper surface, which smooths the surface and removes microscopic roughness .Following the electro-polishing step, the sample is cleaned using acetone and isopropyl alcohol (IPA) to remove any oil residues or organic contaminants from the surface .Finally, the sample is rinsed with deionized (DI) water to eliminate any remaining chemicals, resulting in a clean and smooth copper surface ready for further processing or characterization

3.2 Chemical Preparation Method for graphene

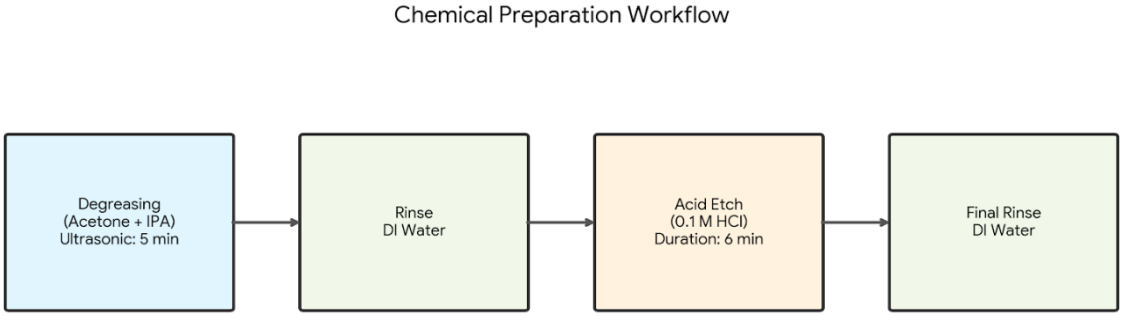

Scheme (2). Chemical preparation workflow for surface cleaning and etching: Degreasing with acetone and IPA (ultrasonic), rinsing with DI water, acid etching with 0.1 M HCl, and final rinse with DI water

This diagram illustrates the chemical surface preparation workflow used to clean and prepare the substrate prior to further processing. Such procedures are commonly applied in materials science and microfabrication to ensure that the surface is free from contaminants and suitable for subsequent experimental steps. Degreasing separately (Acetone and IPA, Ultrasonic Cleaning – 5 mins). The first step involves degreasing the sample using a mixture of acetone and isopropyl alcohol (IPA). Acetone acts as a strong solvent for removing organic contaminants, while IPA assists in dissolving oils and residual impurities. The sample is placed in an ultrasonic bath for 5 minutes, where high-frequency vibrations enhance the cleaning efficiency by dislodging contaminants from the surface. Rinsing with Deionized Water After the degreasing step, the sample is thoroughly rinsed with deionized (DI) water to remove any remaining solvent residues and detached contaminants from the surface. The sample is then subjected to an acid etching treatment using a dilute hydrochloric acid solution (0.1 M HCl) for 6 minutes. This step removes native oxide layers and other surface impurities, thereby improving the surface cleanliness and preparing it for further processing steps. Final Rinse with DI Water Following the acid treatment, the sample is rinsed again with DI water to eliminate any residual acid and reaction byproducts, ensuring a chemically clean surface. Overall, this preparation procedure ensures that the sample

surface is clean, oxide-free, and free from organic contaminants, which is essential for achieving reliable results in subsequent processes such as thin-film deposition, electrochemical measurements, or other surface-related experiment

3.3 Cleaning Si/SiO_2 substrate for MoS_2

Si/SiO_2 is cleaned using acetone followed by isopropyl alcohol (IPA) to remove contaminants. After that, ultrasonic agitation is applied for 5 minutes to enhance cleaning efficiency. Finally, Si/SiO_2 is thoroughly rinsed with deionized (DI) water to remove any residual solvents

3.4 Synthesis of Molybdenum Disulfide (MoS_2)

Pristine MoS_2 was synthesized via a chemical vapor deposition (CVD) method. Sulfur powder (45 mg) and molybdenum trioxide (MoO_3, 10.8 mg) were utilized as precursor components. The growth was conducted in an atmosphere with regulated argon flow and pressure between 50 and 60 Pa. Initially, 50 sccm of argon gas was added. To ensure steady transport conditions during the sulfur sublimation process, the argon flow was first set to 45 sccm for a few minutes and then lowered to 35 sccm. The precursor reaction was started by raising the substrate (Si/SiO_2) temperature to 675°C. Then, it was raised to 750°C, which was maintained for 8 minutes to enable the creation of MoS_2 layers. The system was naturally cooled to room temperature in an argon environment following the reaction.

3.5 Synthesis of Graphene

Graphene was synthesized using a plasma-assisted chemical vapor deposition (PECVD) process. Initially, the substrate was annealed at 950 °C for 50 mins under a continuous flow of argon (Ar) gas at 80-100 sccm to remove surface impurities and improve the crystallinity of the catalytic surface. After the annealing step, the furnace temperature was gradually reduced to the growth set point of 850 °C. During the growth stage, a gas mixture consisting of argon (Ar, 31 sccm) and methane (CH_4, 2 sccm) was introduced into the reaction chamber as the carrier and carbon precursor gases, respectively. A plasma cloud created by forward power of 25 W, Radio Frequency 13.6 MHz in an Auto-matching mode was applied for 10 min to activate the methane molecules and promote the decomposition of the carbon precursor, facilitating the nucleation and growth of graphene layers on the substrate surface. The distance between the plasma edge and the substrate center was maintained at approximately 30 cm to ensure a uniform plasma distribution during the growth process. The environmental pressure was controlled and maintained within the range of 45–47 Pa throughout the synthesis process.

4. Results and Discussion

4.1 Cu Foil Substrate Characterization

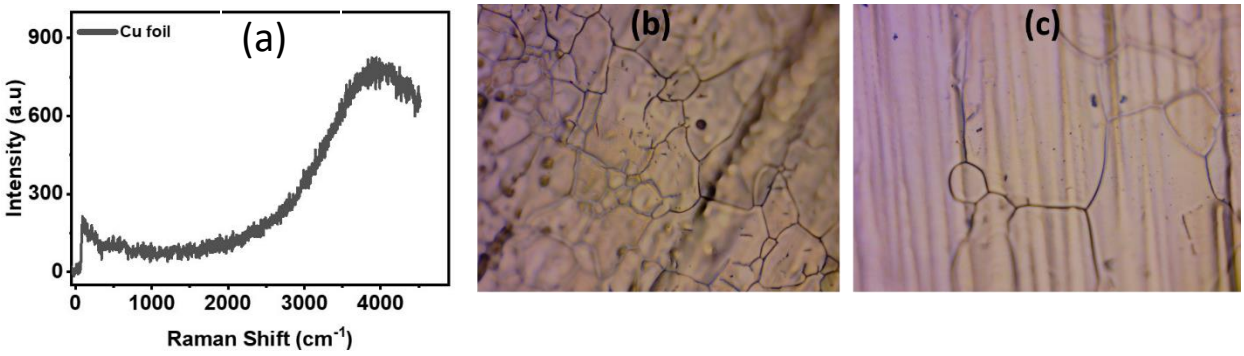

Fig.1 Characterization of the pristine Cu foil surface before growing graphene

Fig1 (a) Raman spectrum of the copper foil after electropolishing and subsequent annealing, showing a smooth response without any additional peaks related to copper oxide species, indicating that the surface consists of metallic Cu with no detectable oxidation. (b) Optical

microscopy image after electropolishing and annealing, revealing the typical polycrystalline grain structure of the copper foil. The grains and grain boundaries are clearly visible, with no evidence of oxide particles or corrosion features on the surface. (c) Surface morphology of the chemically polished Cu foil after annealing. The observed parallel polishing lines originate from the mechanical preparation process. The surface remains uniform and oxide-free, confirming that the substrate is pure copper after the annealing process.

4.2 Graphene Characterization

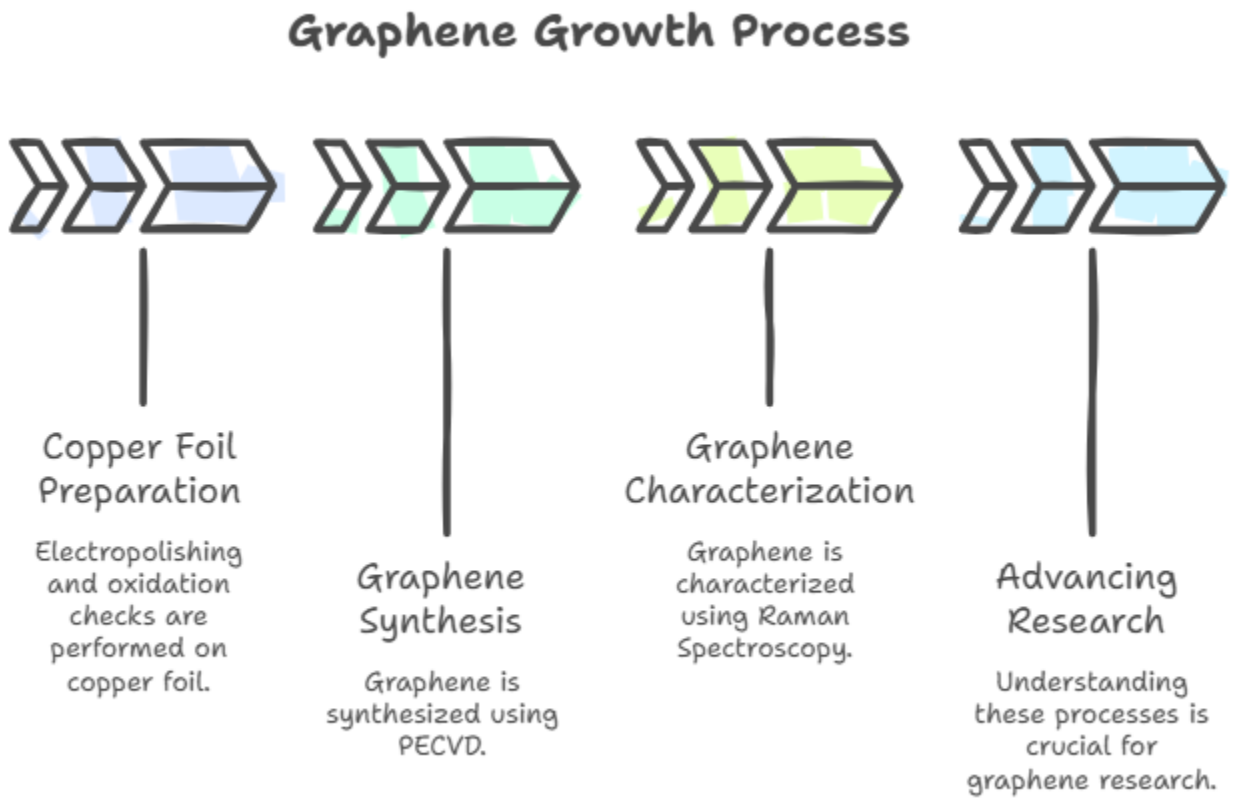

Scheme (3). Schematic illustration of graphene preparation via electropolishing of the copper substrate followed by (PECVD) growth. Raman spectroscopy is used before and after growth to confirm the absence of oxidation and to evaluate the quality of the synthesized graphene.

The schematic illustration presents the sequential process used for the preparation and characterization of graphene. Initially, the copper substrate undergoes electropolishing to

improve surface smoothness and remove surface contaminants. In this step, the copper foil is immersed in an electrolyte solution and subjected to an applied electrical potential, resulting in the controlled dissolution of surface irregularities and the formation of a highly smooth and clean surface suitable for subsequent growth processes. After the electropolishing step, Raman spectroscopy is employed to verify the chemical state of the substrate and confirm the absence of oxidation. The Raman spectrum is examined to ensure that no oxide-related features are present, indicating that the copper surface remains metallic and suitable for high-quality graphene growth. Following substrate preparation and verification, graphene is synthesized using the chemical vapor deposition (CVD) technique. During this process, hydrocarbon precursor gases decompose at elevated temperatures on the copper surface, leading to the nucleation and growth of graphene layers. The copper substrate acts as a catalytic surface that facilitates the formation of a uniform graphene film. Finally, the quality and structural characteristics of the synthesized graphene are evaluated using Raman spectroscopy. The Raman spectrum typically shows characteristic D, G, and 2D peaks, which provide information about the structural order and defect density of the graphene layer. In particular, the intensity ratio between the D and G bands (ID/IG) is used to assess the defect level in the graphene structure, where a lower ratio indicates higher crystallinity and better graphene quality. Overall, this workflow ensures the preparation of a clean copper surface, controlled graphene growth via CVD, and reliable characterization using Raman spectroscopy to confirm the structural quality of the resulting graphene

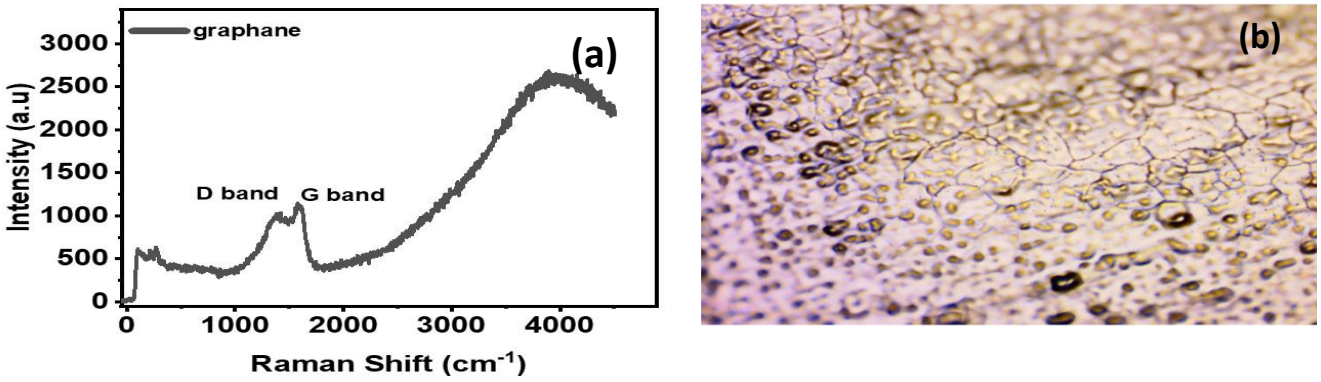

Fig 2. (a) Raman spectrum of the synthesized graphene (b) Optical microscopy image of the prepared graphene film illustrating the surface morphology and the distribution of graphene domains over the substrate.

In part (a), the Raman spectrum shows the D band (~1350 cm^{-1}) and G band (~1580 cm^{-1}). The D band indicates defects or structural disorder in the graphene, while the G band corresponds to the in-plane vibrations of sp^2 carbon atoms. The absence of the 2D band (~2700 cm^{-1}) suggests the graphene is multilayered or has structural imperfections. Part (b) is an optical microscopy image illustrating the surface morphology and distribution of graphene domains across the substrate, giving insight into the coverage and uniformity of the prepared graphene film.

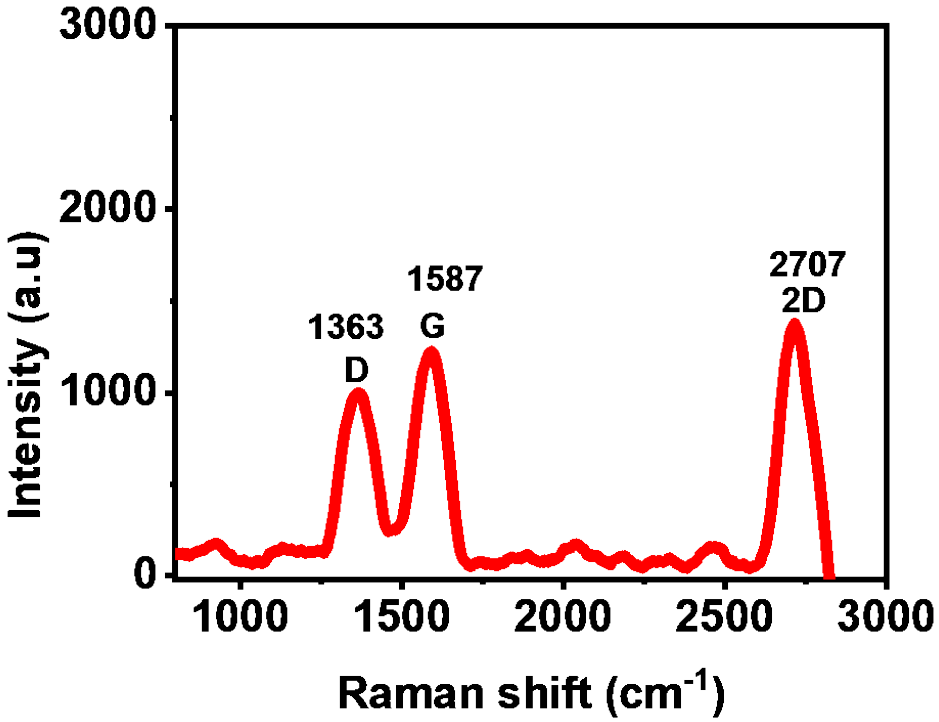

Fig.3 Raman spectrum of graphene showing the characteristic of graphitic form

Fig.3 shows the Raman spectrum of the PECVD-grown carbon film, exhibiting three characteristic peaks at approximately 1363 cm^{-1} (D band), 1587 cm^{-1} (G band), and 2707 cm^{-1} (2D band). The G band corresponds to the in-plane vibrational mode of sp^2-bonded carbon, confirming the development of a graphitic carbon network. The pronounced D band indicates disorder-activated scattering, resulting from defects, grain boundaries, edge sites, and/or residual amorphous carbon. In well-crystallized graphite, the D band is typically weak; thus, the clearly observable D peak here suggests that the deposited film is not highly ordered graphite but rather nanocrystalline/defective graphitic (graphene-like) carbon, commonly formed under non-optimized CVD conditions. The appearance of the 2D band further supports the presence of sp^2

carbon; however, the overall lineshape and the defect-activated D response indicate limited crystalline domain size and substantial structural disorder. To enhance graphitization and decrease defect density, the CVD process can be optimized by lowering the precursor partial flow (sccm), raising the growth temperature, improving catalyst (e.g., Cu/Ni) pre-annealing in H_2/Ar to reduce nucleation density, and utilizing post-growth annealing in an inert/reducing atmosphere, which together promote larger sp^2 domains and mitigate amorphous carbon formation

4.3 MoS_2 Characterization

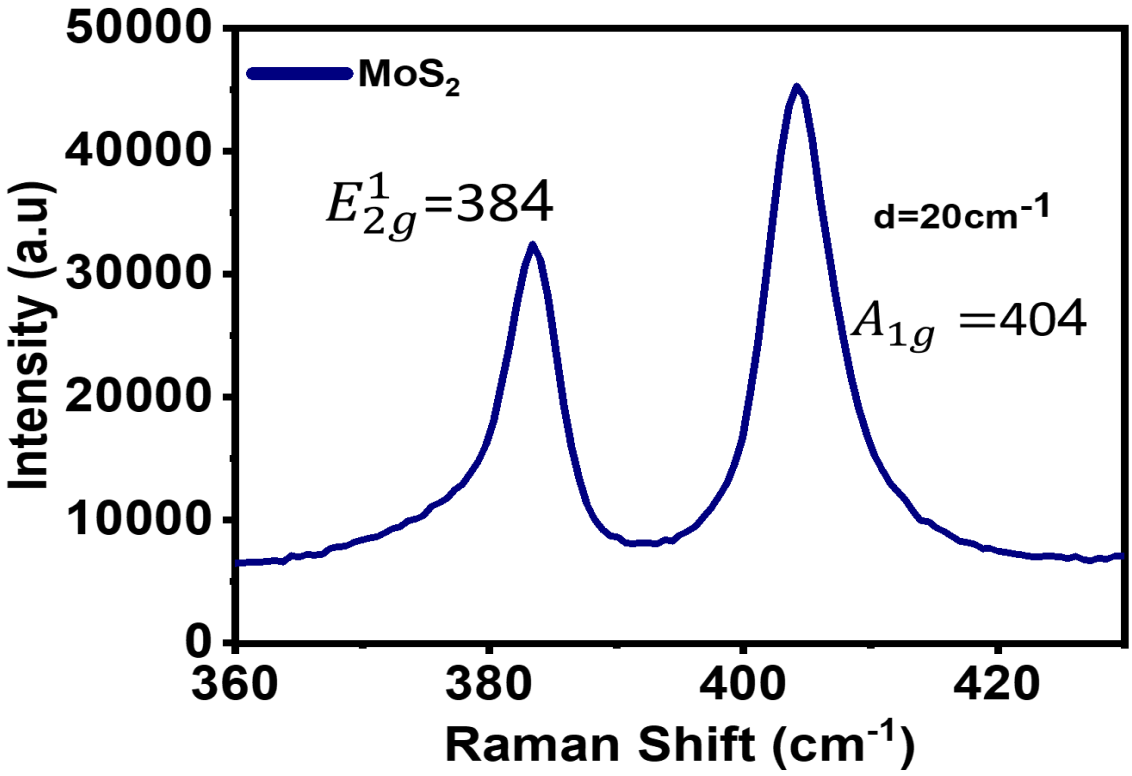

Fig.4 Raman spectra of MoS_2

The Raman spectrum of the synthesized MoS_2 sample exhibits two prominent characteristic peaks located at approximately 384 cm^{-1} and 404 cm^{-1}, which correspond to the E^2g^1 and A^1g vibrational modes, respectively. These two Raman-active modes are well known fingerprints of layered molybdenum disulfide. The E^2g^1 mode originates from the in-plane vibration of molybdenum (Mo) and sulfur (S) atoms, where both atoms vibrate in opposite directions within the basal plane of the layered structure. In contrast, the A1g mode is attributed to the out-of-plane vibration of

sulfur atoms, in which the sulfur atoms oscillate perpendicular to the MoS_2 layers. The frequency difference between these two peaks (d = A1g − E2g¹) is an important parameter for determining the number of MoS_2 layers. In the present spectrum, the peak separation is approximately 20 cm^{-1}, which is typically associated with few-layer MoS_2 rather than bulk material or monolayer structures. It is well established that the separation between these two modes increases with the number of layers due to enhanced interlayer van der Waals interactions. The clear appearance of these two characteristic Raman modes and their separation confirms the successful formation of layered MoS_2 with a few-layer structure. Furthermore, the sharpness and high intensity of the peaks indicate a good crystalline quality of the synthesized material.

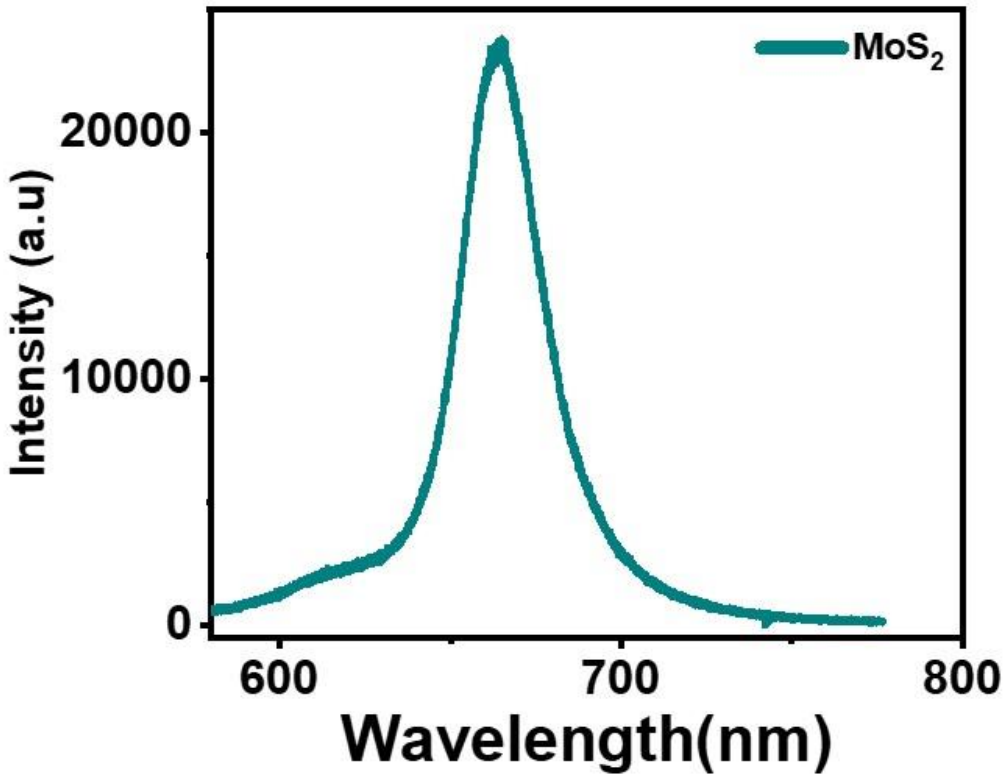

Fig.5 The PL of MoS_2

In the fig.5 The PL spectrum of few-layer MoS_2 exhibits a dominant emission centered at ~660–670 nm (≈1.85–1.90 eV), which is attributed primarily to the A-exciton transition associated with the direct optical transition at the K point. Although this excitonic feature remains observable in few-layer MoS_2, the PL efficiency is generally reduced relative to monolayer due to the increasing contribution of an indirect band gap and enhanced non-radiative/phonon-assisted recombination

channels. The broadened emission profile may indicate inhomogeneous broadening arising from thickness non-uniformity, strain, and/or spectral overlap with charged excitons (trions) and defect-related emissive states.

5. Conclusion

In this work, copper foil substrates were prepared using two different surface treatment methods: electropolishing and chemical treatment. These preparation techniques aimed to enhance the surface quality of the copper foil and ensure optimal conditions for subsequent material growth. Raman spectroscopy measurements were first conducted on the copper foil to assess the surface condition and confirm its suitability for further processing. Following substrate preparation, graphene was successfully synthesized on the copper foil using the Plasma-Enhanced Chemical Vapor Deposition (PECVD) method. In contrast, MoS_2 was grown on Si/SiO_2 substrate under similar CVD conditions. This approach allowed for the controlled growth of high-quality two-dimensional materials on their respective suitable substrates. Raman spectroscopy was then employed as a characterization tool to validate the successful synthesis and structural quality of the prepared materials. The Raman spectra confirmed the presence of the characteristic vibrational modes of both graphene and MoS_2, demonstrating their successful growth and good structural quality. Overall, this study highlights the effectiveness of substrate preparation methods combined with PECVD growth and Raman spectroscopy as a reliable approach for the synthesis and characterization of two-dimensional material

6. Acknowledgements

My sincere gratitude goes to Prof. Dr. Grigory Arzumanyan, my supervisor, for granting me the valuable opportunity to participate in the START program. His continuous guidance and support allowed me to benefit from his extensive expertise and gain significant scientific and practical experience throughout this journey. Special appreciation is extended to Kahramon Mamatkulov, the group leader, for his leadership and for fostering a supportive and collaborative environment during the program. I am particularly grateful to Khlood A. A. Abdeljawaad for her exceptional support and generosity in sharing her knowledge and experience. Her guidance played an important role in helping me develop new skills and gain valuable experience. I am especially thankful for her support during the application process and for her continuous encouragement, which greatly enriched my learning journey. My appreciation also goes to Le Duc Huy, my task leader, for his guidance, coordination, and helpful feedback throughout the project. Sincere thanks are also extended to Yersultan Arynbek and Pham Ngoc Bao Tri for their cooperation and support within the group I would like to sincerely thank Aizhan Damir and Makhfuza Eshonqulova for their valuable assistance and support during the laboratory work, and which made the teamwork experience both productive and enjoyable. I am deeply grateful to everyone who contributed to making this experience both valuable and memorable.

7.References

1. Alqarni, L.S. and M.D. Alghamdi, *Graphene and its derivatives as surface-enhanced Raman spectroscopy substrates for glucose detection.* Journal of Science: Advanced Materials and Devices, 2025. **10**(4).
2. Chauhan, S., L. Gupta, and S. Sharma, *A systematic review on the analysis of trace materials via Raman spectroscopy: Advancements and forensic implications.* Forensic Sci Int, 2025. **377**: p. 112609.
3. Fernandez, C.J., et al., *Confocal Raman spectroscopy applied to microemulsions and nanoemulsions.* Current Opinion in Colloid & Interface Science, 2025. **78**.
4. Hou, Z., et al., *Surface-enhanced Raman spectroscopy for Alzheimer's Disease biomarkers detection: Advances, challenges, and future perspectives.* Thermochimica Acta, 2026. **757**.
5. Kurek, A., et al., *Analysis of red blood cells from individuals with allergy symptoms using Raman spectroscopy.* Journal of Molecular Structure, 2026. **1352**.
6. Luo, A., et al., *Advances in Raman spectroscopy for in vivo imaging.* TrAC Trends in Analytical Chemistry, 2026. **198**.
7. Ma, F., et al., *Recent advances in chiral recognition based on surface-enhanced Raman scattering spectroscopy.* Chinese Chemical Letters, 2026. **37**(4).
8. Madatov, R.S., et al., *Study of the effect of ionizing γ-radiation on the structural and vibrational properties of GaS and Yb-doped GaS (GaSYb) single crystals by X-ray diffraction (XRD) and Raman spectroscopy.* Radiation Physics and Chemistry, 2026. **240**.
9. Wang, L.-X., et al., *Research applications of Raman spectroscopy and Raman imaging for fingermark analysis.* Science & Justice, 2026. **66**(2).
10. Zhang, H., et al., *Raman spectroscopy as the quantum eye to reveal molecular dynamics in biology.* Adv Colloid Interface Sci, 2026. **351**: p. 103805.
11. Zhang, Q., et al., *Surface-enhanced Raman spectroscopy for protein detection: Challenges and countermeasures.* Talanta, 2026. **298**(Pt A): p. 128901.
12. Zhu, W., et al., *Structural regulation of 1T-MoS2/Graphene composite materials for high-performance lithium-ion capacitors.* Journal of Energy Storage, 2024. **102**.
13. Badiger, J.G., et al., *Stabilizing metastable 1T MoS2 via electrochemical proton intercalation for hydrogen evolution reaction.* Journal of Power Sources, 2025. **652**.
14. Jia, Q., et al., *Microstructure regulation of 1T-MoS2 via polyethylenepolypropylene glycol and ethanol treatment for high-stability supercapacitor.* Journal of Energy Storage, 2025. **110**.
15. Kang, M., et al., *Reduced graphene oxide-intercalated MoS2 nanoflowers cathode for aluminum-ion batteries.* Chemical Engineering Journal, 2025. **520**.
16. Ling, D., D. Zhang, and Q. Wang, *Interfacial electric field modulation of WS2/MoS2 hollow nanosphere heterostructures for enhanced ammonium-ion asymmetric supercapacitor.* Chemical Engineering Journal, 2025. **520**.
17. Sun, D., et al., *1T MoS2 nanosheets with extraordinary sodium storage properties via thermal-driven ion intercalation assisted exfoliation of bulky MoS2.* Nano Energy, 2019. **61**: p. 361-369.
18. Niu, H., et al., *Structurally stable ultrathin 1T-2H MoS2 heterostructures coaxially aligned on carbon nanofibers toward superhigh-energy-density supercapacitor and enhanced electrocatalysis.* Chemical Engineering Journal, 2020. **399**.
19. Xu, C., et al., *Miniaturized high-performance metallic 1T-Phase MoS2 micro-supercapacitors fabricated by temporally shaped femtosecond pulses.* Nano Energy, 2020. **67**.
20. Lee, S., et al., *Oxygen incorporated in 1T/2H hybrid MoS2 nanoflowers prepared from molybdenum blue solution for asymmetric supercapacitor applications.* Chemical Engineering Journal, 2021. **419**.
21. Lien, C.-W., et al., *Optimization of acetonitrile/water content in hybrid deep eutectic solvent for graphene/MoS2 hydrogel-based supercapacitors.* Chemical Engineering Journal, 2021. **405**.